RSC Advances

PAPER

View Article Online
View Journal | View Issue

Cite this: *RSC Adv.*, 2024, **14**, 8502

Development of hybrid electrospun alginate-pulverized moringa composites

Abimbola Oluwatayo Orisawayi, *[ab] Krzysztof Koziol,[a] Shuai Hao,[a] Shivam Tiwari[a] and Sameer S. Rahatekar*[ab]

The consideration of biopolymers with natural products offers promising and effective materials with intrinsic and extrinsic properties that are utilized in several applications. Electrospinning is a method known for its unique and efficient performance in developing polymer-based nanofibers with tunable and diverse properties presented as good surface area, morphology, porosity, and fiber diameters during fabrication. In this work, we have developed an electrospun sodium alginate (SA) incorporated with pulverized *Moringa oleifera* seed powder (PMO) as a potential natural biosorbent material for water treatment applications. The developed fibers when observed using a scanning electron microscope (SEM), presented pure sodium alginate with smooth fiber (SAF) characteristics of an average diameter of about 515.09 nm (±114.33). Addition of pulverized *Moringa oleifera* at 0.5%, 2%, 4%, 6%, and 8% (w/w) reduces the fiber diameter to an average of about 240 nm with a few spindle-like pulverized *Moringa oleifera* particles beads of 300 nm (±77.97) 0.5% particle size and 110 nm (±32.19) with the clear observation of rougher spindle-like pulverized *Moringa oleifera* particle beads of 680 nm (±131.77) at 8% of alginate/*Moringa oleifera* fiber (AMF). The results from the rheology presented characteristic shear-thinning or pseudoplastic behaviour with a decline in viscosity, with characteristic behaviour as the shear rate increases, indicative of an ideal polymer solution suitable for the spinning process. Fourier transform infrared spectroscopy (FT-IR) shows the presence of amine and amide functional groups are prevalent on the alginate-impregnated moringa with water stability nanofibers and thermogravimetric analysis (TGA) with change in degradation properties in a clear indication and successful incorporation of the *Moringa oleifera* in the electrospun fiber. The key findings from this study position nanofibers as sustainable composites fiber for potential applications in water treatment, especifically heavy metal adsorption.

Received 7th January 2024
Accepted 7th March 2024

DOI: 10.1039/d4ra00162a

rsc.li/rsc-advances

1. Introduction

The novelty and improvement in polymer science, engineering, and materials chemistry have made the progress of polymeric nanofibers through the electrospinning process an interesting and suitably sustainable method in the membrane fabrication field for researchers. It presents an excellent means of producing a unique three-dimensional network using minimal solvent to improve material properties and applications.[1] Such properties involve high surface area, and mechanical properties, well-structured membrane porosity, excellent electrical conductivity, variable pore size, and thermal properties.[2,3] Furthermore, polymer nanofibers with sizes ranging from various microns to millimicrons have been used to encapsulate natural cues, such as antibiotics, antitumor agents, proteins, natural and sustainable products, and growth factors for several applications, water treatment, including energy, and healthcare.[4]

Electrospinning is a unique advanced engineering method for developing micro or nano-structured products using polymer solutions that can be stretched into fibers.[5,6] By utilizing electrostatic force to generate a fibrous covering of several membrane layers.[7] The use of multi-fluid electrospinning has also been an advanced engineering technique with an enhanced potential to create innovative functional micro and nano-materials.[8] It is suitable for a combination of varied materials to form complex inner-structured structures with special surface characteristics of components, and compositions.[8] The setup consists of a very high-voltage source by the application of positive and negative charged connections, well-regulated pumps, a spinneret for loading the polymer solution, and a known collector with either a rotary or stationary plate[9,10] Findings have shown that the nature of the membrane

[a]*Composites and Advanced Materials Centre, School of Aerospace, Transport, and Manufacturing, Cranfield University, Bedfordshire MK43 0AL, UK. E-mail: abimbola.orisawayi@cranfield.ac.uk; ao.orisawayi@oaustech.edu.ng; bimboris_t@yahoo.com; S.S.Rahatekar@cranfield.ac.uk*

[b]*Department of Mechanical Engineering, School of Engineering and Engineering Technology Olusegun Agagu University of Science and Technology, (OAUSTECH), Okitipupa, Nigeria*

developed can be influenced by the type of collector plate used during the process. For example, membranes formed on motionless stationary assembling collector plates sometimes develop a permeable random porous structure, while those developed on the normal rotary wet or dry collector plates may usually exhibit a well-organized 3-dimensional (3-D) architecture.[11–15] Studies conducted by Topuz *et al.* on a super oleophilic oil-adsorbing type of membranes used for porous and nonporous fluorinated polyimides were also used for the rapid remediation of oil spills and the membrane was also hydrophobic, showcasing high oil adsorption capacities for adsorbing various oils.[16]

Other studies using electrospinning in water studies were in the development of membranes used in various separation techniques, such as microfiltration, absorption, adsorption, absorption, ultrafiltration, nanofiltration, and techniques involved in the reverse osmosis and forward osmosis technologies.[17–19] Further studies may include some medical activities such as wound dressing, healing technology, and pharmaceuticals industries such as drug deliveries[20–22] and studies on developing infiltration and new material development, energy storage and sound absorption, fuel cells, and tissue engineering, among others[23,24]

In recent decades, mostly artificial polymers have been extensively used in the development of nanofiber inventions. However, the challenges with these uses are biodegradation and requiring poisonous or toxic solvents to form the solutions during production leading to environmental issues such as contamination affecting water bodies and aquatic life and its environments. Studies have also revealed that the use of photocatalysts for water decontamination can be expensive and may develop secondary pollution to aquatic life.[25–28] Therefore, there is a need to consider novel, bio-based, affordable, environmentally friendly, and sustainable non-toxic polymeric membrane composites.[29]

Alginates are some of the most recognized naturally occurring, biodegradable polysaccharides consisting of anionic polymers extracted from seaweed. It has attracted significant interest from researchers due to its distinctive properties, such as low toxicity, biocompatibility, availability, and gelation induced by the addition of divalent cations such as Calcium ion (Ca^{2+}). These properties make alginate suitable for water treatments specifically in heavy metals removal, coagulation, and antibacterials.[30,31] Alginate is water-soluble and characterized by its linear copolymer composition of β-D-mannuronic acid, referred to as M-blocks, and is also identified by α-L-guluronic acid, known as G-blocks, with monomers typically linked by β-(1–4) glycosidic bonds.[32] Current reports suggest that most naturally occurring polymers including alginate are known for their difficulty in electrospinning from their aqueous solutions due to their high viscosity, and form gels in aqueous solutions due to hydrogen bonding.[33,34] To address this challenge, synthetic polymers such as polylactic acid (PLA), polyvinyl alcohol (PVA), and polyethylene oxide (PEO) which are water-soluble, are often employed to enhance the electrospinning process.[32,35,36]

Several works have been done on the electrospinning of alginate for various applications and have been proven successful. Among these works, studies on the use of essential oils produced from oregano oils blended with specific types of medium molecular alginate to develop an antimicrobial electrospun composite for wound healing applications.[37] Additionally, some studies have developed biobased nonwoven mats containing protein extracts and baicalein extracted from Chinese herbs, for wound healing applications.[38] Alginate was also combined with soybean protein nanofibers potentially to be used for biomedical applications.[39]

Moringa oleifera plant is a medium-sized plant thriving globally and adapts in many tropical in most tropical and subtropical regions, but studies described its origin to be traced back to Afghanistan, Bangladesh, India, and Pakistan. The seed has several applications for pharmaceutical and Traditional purposes such as a cure for wounds and healing, pains, kidney cleansing, liver diseases, heart failure disease, cancer treatment, and ulcer inflammation.[40] *Moringa oleifera* is also a source of food nutrition, and cosmetics industries, with many other applications and unique properties.[41–43]

Studies have been considering the potential of bending the moringa seed powder and pyrolyzing the seed husk for water treatment applications, most especially in developing countries, because of its availability, many communities explore the prospect of using it for the treatment of water from different sources form rivers, waterways, and streams.[44] *Moringa oleifera* seeds were reported to have proven to treat water as a coagulant due to positively charged, water-soluble proteins prevalent in the seeds, which bind with most negatively charged water sediments (silt, clay, bacteria, toxins, *etc.*),[45] There are also indications of antimicrobial agents and heavy metals removal. Treatments with Moringa solution remove about 90 to 99.9% of the impurities in the water reported.[46,47]

The current work uses an electrospinning technique to develop alginate-pulverized *Moringa oleifera*-based electrospun nanofibers. The concentration of the *Moringa oleifera* is varied and the developed fibers are characterized to analyse the effect of moringa on the electrospun fiber mats and its potential application in water-treatment applications.

2. Experimental methods and materials

2.1 Materials and methods

Sodium Alginate SA from Brown algae, viscosity 5.0–40.0 cps $c =$ 1%, was obtained from Sigma-Aldrich, poly(ethylene oxide) (PEO) M.W. 1 000 000 powder was purchased from Thermo Fisher Scientific, Alfa Aesar (USA), calcium chloride ($CaCl_2$) (anhydrous, granular, ≤7.0 mm, ≥93.0%, *d*: 2.15 g cm^{-3}, Sigma-Aldrich, China), and *Moringa oleifera* seed was purchased from an African Market (Locally Sourced).

2.2 Preparation of PEO/alginate solution

The SA (8 wt%) and PEO (4 wt%) were dissolved separately in deionized water for 24 hours to ensure complete dissolution.

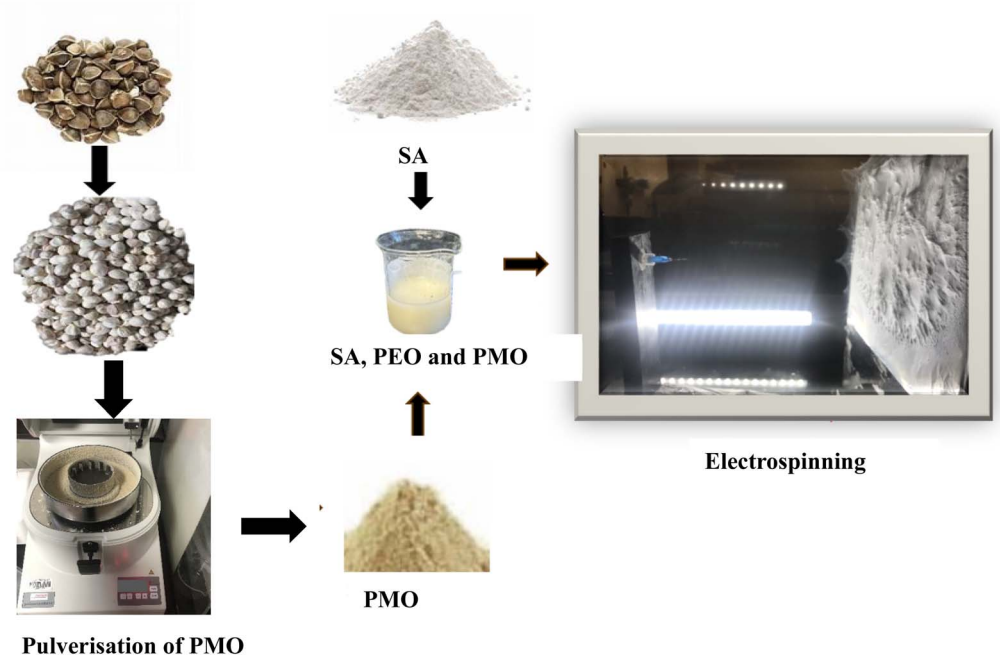

Fig. 1 Schematic preparation of fabrication of SA loaded with PMO through electrospinning process.

The SA and PEO aqueous solutions were then mixed at 80 : 20 ratios and stirred for an additional 4 hours to ensure homogeneity at room temperature before the electrospinning experiment.

2.3 Extraction methods of the PMO

The *Moringa oleifera* seed used in this study were sourced without pods from a reputable pure organic seller "Purely Agro DGT Limited 275 New North Road London." The shell was removed manually(de-shell) to obtain the seed. The seed samples were dried in the vacuum oven at 65 °C for 24 hours to remove and reduce the moisture content.[48] The dried sample was stored at room temperature in polyethylene bottles in a desiccator for preservation before use.[49] The dried moringa seed was pulverized in a high-speed PULVERISETTE 14 instrument shown in Fig. 1. The pulverized process was about 4–5 minutes at a speed between 6000 and 10 000 rpm using an available sieve mesh ring or cassette of 2 mm in the laboratory until desirable samples were obtained.

2.4 Preparation of SA, PMO and PEO

The SA and PEO were prepared separately and dissolved in deionized water for 24 hours to ensure complete homogeneity. As part of optimizing solution parameters, the concentration of the blend was varied with different concentrations of *Moringa oleifera* suspension to the addition of 8 wt% SA added to the *Moringa oleifera* suspension dose of 100 ml of distilled water at 0.5%, 1%, 2%, 4%, 6%, and 8% each was mixed with 4% PEO. The ratio of SA, PMO and PEO is 80 : 20 and the blends were stirred with a magnetic stirrer for 4 hours to enable good Spinnability.

2.5 Electrospinning process

Electrospinning instrument FLUIDNATEK™ Machine LE-50 consisting of pumps, high voltage source, and collector plated built in an electrospinning chamber developed by Bioinicia, Valencia, Spain was used to develop the fiber membrane. Earlier before the experimentations, the composition of pure SA, PEO, and SA, PMO, PEO solutions were loaded separately into the syringe, and the needle was attached according to the manufacturer's description in the user's manual. A dry aluminium foil was mounted on the surface of the stationary plate connector for the sample collection. Individually sample was electrospun for the same volume (10 ml) using the electrospinning parameters 0.4 mm needle, the flow rate of 1.0–1.2 μl h^{-1}, at room temperature, and relative humidity of 40–60% and stationary dry collector kept at 15 cm, the voltage was adjusted until Taylor's cone was at the tip of the needle, the observed voltage was about 23–24 kV A. Fig. 1 shows a schematic representation of the blended solutions and nanofiber fabrication through electrospinning process of SA, PEO and PMO.

2.6 Crosslinking process

After the electrospinning experiment, the aluminium foil was removed from the machine collector's plate and the samples were immersed in a freshly prepared 4% $CaCl_2$ solution for about 10 min. The developed fiber membrane was then removed from the foil with a tweezer (Fig. 2), washed severally in deionized water, and later immersed in deionized water for 24 hours. The samples were later dried in the open air at room temperature and further dried in the vacuum oven at 40 °C for 2 hours to remove moisture before characterization.

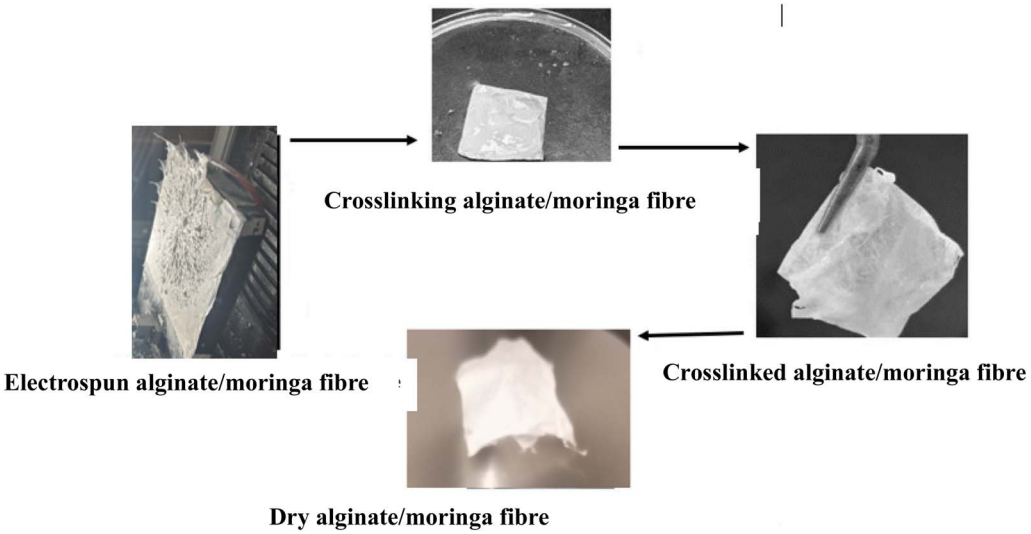

Fig. 2 A simple crosslinking process of SA loaded with PMO.

3. Experimental

3.1 Fourier transforms infrared (FTIR)

The Fourier transform infrared (FTIR) characterisation of the samples was conducted on the Nicolet iS10 FTIR Spectrometer equipment with an inbuilt Attenuated Total Reflectance (ATR) fixture designed by Thermo Fisher Scientific™, Verona, Madison, USA. The spectral of the samples was collected in the wavenumbers ranging between 4000 and 500 cm^{-1} at 50 scans with a resolution of 4 cm^{-1} at room temperature, Using supported OMIC Software. These analytical methods investigate the PMO, SA, and AMF.

3.2 Rheology

The rheology characterisation was done on AR-2000ex (TA instruments)8F382@lab fitted with standard steel parallel plate with the geometry of 40 mm (SST) description was used, calibrated with rotational mapping with three iterations, adjusted manually with a gap of the upper geometry within 5 mm of the lower gap without a solvent gap, the geometric inertial of the calibration was about 3.681 ($\mu N\ m\ s^2$) at temperature room temperature set at 25 °C on the instrument. A flow step flow experiment was conducted. The experiment was done on freshly prepared samples of a volume of 1.26 ml used for a single experiment. The shear viscosity was measured at 0.01–1000 s^{-1} range of shear rate with 30 data points.

3.3 Scanning electron microscope (SEM)

The morphologies of individual fiber membranes were determined using a scanning electron microscope 'S8000, (ESEM) (TESCAN, Kohoutovice, Czech Republic). Samples of about 5 mg were mounted on the sample holder and coated with AU10 (gold).

3.4 Thermogravimetric analysis (TGA)

The thermogravimetric analysis was conducted on TGA A5500 Thermogravimetric Analyzer from TA instrument, USA, using the platinum pan and Ambient to 1000 °C using the Trios Software. The samples were dried in the vacuum oven at about 40 °C for about 2 hours, the samples were measured and about 5 mg of each sample were loaded in the dynamic mode and heated from room temperature to 800 °C at a rate of 10 °C min^{-1}, under a nitrogen atmosphere.

4. Result and discussion

4.1 Fourier transform infrared (FTIR)

FTIR analysis was performed on the chemical composition of samples of the sodium alginate SA, PMO, and AMF shown in Fig. 3. The spectrum of pure SA was studied and compared with the results from several works of literature. The peaks of SA as shown in Fig. 3 appeared as compared same as a common broad peak at 3700–3000 cm^{-1} can be attributed to –OH stretching vibration, low-intensity bands at about 2900 cm^{-1} attributed to –CH_2 groups, and at 1597 and 1409 cm^{-1} are attributes of asymmetric and symmetric stretching modes, of carboxylate salt groups (–COONa) in the sodium alginate.[50–52] In the PMO, spectra also show an exceptionally good attribute compared to the literature. The broadband focused at 3419 cm^{-1} can be ascribed to O–H stretching which appears mainly or connected to proteins, carbohydrates, and fatty acids, and the lignin unit structure existence ascribed to the high protein content, there is also a trait of N–H stretching of amide groups in this region.[53] The peaks that appear at 2925 and 2855 cm^{-1} correspond respectively to the asymmetric and symmetric stretching of the characteristics or connection of –CH in the CH_2 group.[48,54] The presented intensity of these bands could be related to the numerous proportions of the protein reported by.[48,55,56] The overlapping band's spectrum presented between 1747 and 1658 cm^{-1} can be ascribed to the C=O connection stretching. The two bands of 1658 and 1747 cm^{-1} can be attributed and reported as related to the carbonyl group being present in the fatty acid and protein structures associated with fatty acids and

a band at 1546 cm^{-1} related to the amide group in the protein content of the *Moringa oleifera* seed. The peak at 1468 cm^{-1} can be allocated to the reported C–N stretching or/and that of the N–H deformation.[49] The presence of this band is often related and confirmed as compared with literature to be related to the protein structure in the PMO. The stretching vibrations located between 722 and 500 cm^{-1} represent C–H, C=C, and N–H. A report by Araújo *et al.* shows that *Moringa oleifera* seeds present a protein mass composition of about 29.36 g/100 g of the seeds.[48]

The spectrum of the alginate/*Moringa oleifera* fibre (AMF) product was compared with previous studies from moringa functionalized alginate studied by Militao *et al.* The broadband was cantered at 3384 cm^{-1}, which can be allocated to the O–H stretching of proteins as compared with as well as carbohydrates in alginic acid from the alginate studied by.[57–62] The peaks at 2889 and 2820 cm^{-1} respectively correspond to the asymmetric and symmetric stretching of the C–H in the $-CH_2$ protein group.[63] The peaks at 1746 cm^{-1} and 1605 cm^{-1} were assigned to have the attributes of carbonyl that may be linked to the amides of protein or fatty acid from lipids as reported in the spectrum of the *Moringa oleifera*. The final FTIR spectra show clear indication and successful incorporation of the *Moringa oleifera* in the electrospun fiber.

4.2 Rheology characterisation

The viscosity of a solution plays a crucial role in the determination of the spinnability of a solution during the electrospinning process[64] in exploring this phenomenon to understand how the preparation of the solution influences the spinnability of the resultant membrane. Previous research has indicated that certain biopolymers, like alginate, face challenges in electrospinning.[65,66] This limitation often necessitates the addition of polymers such as PEO to improve the spinnability. Fig. 4 presents the flow curve, explaining the interactions between SA, PEO, and the effects of incorporating PMO at varying concentrations. From the flow curve, there is a notable observation with a significant reduction in viscosity upon the addition of PEO to the primary solution. This reduction can be attributed to the lower concentration of 4% PEO compared to SA at 8%, which is influential in facilitating optimal fiber formation as observed from the SEM. Fascinatingly, introducing 0.5% of PMO further reduces the solution's viscosity. This phenomenon might be linked to the solubility of certain components in the PMO, such as the soluble proteins, carbohydrates, fatty acids, and oils inherent in the pulverized *Moringa oleifera* seeds. The rheological results for concentrations of 0.5%, 4%, and 8% wt were chosen based on favourable morphology, as

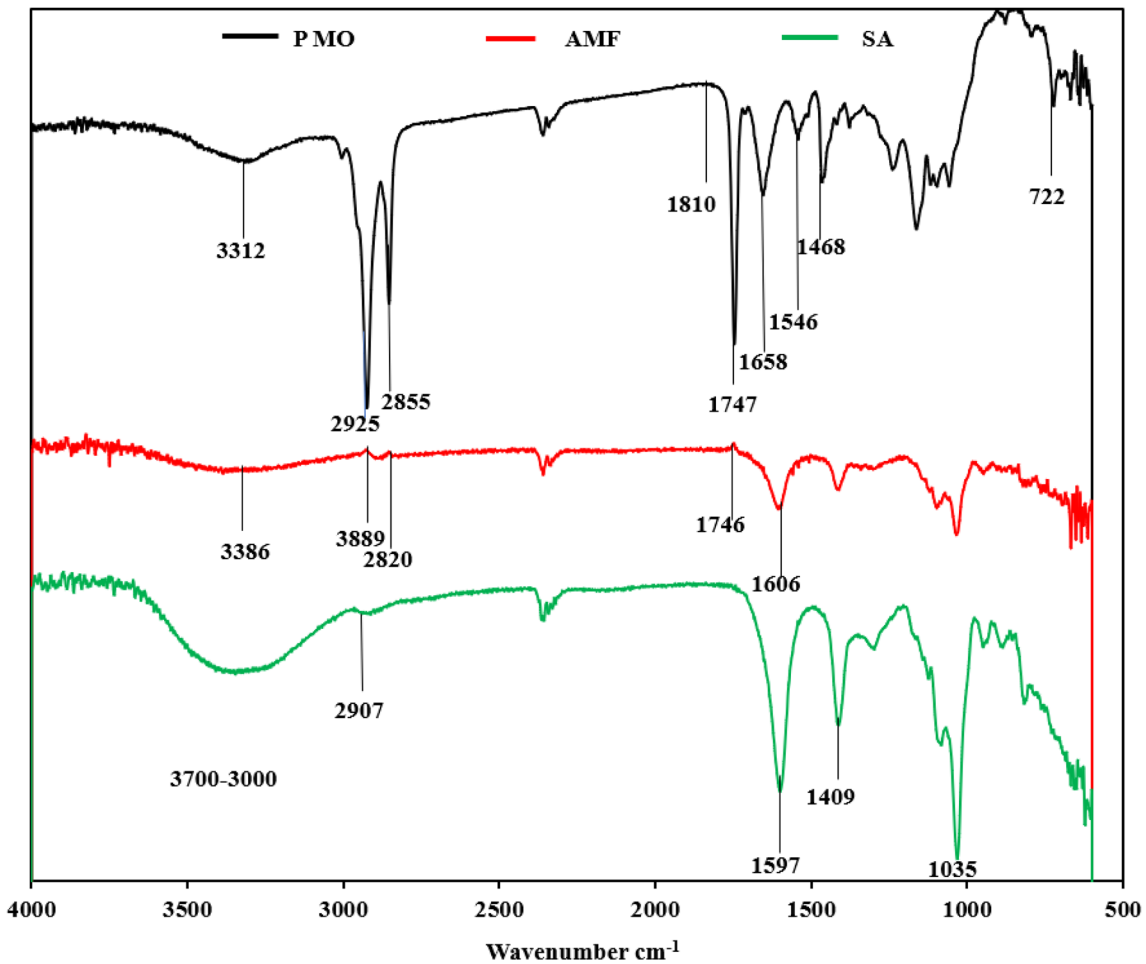

Fig. 3 FT-IR spectra of PMO, SA, and AMF shown.

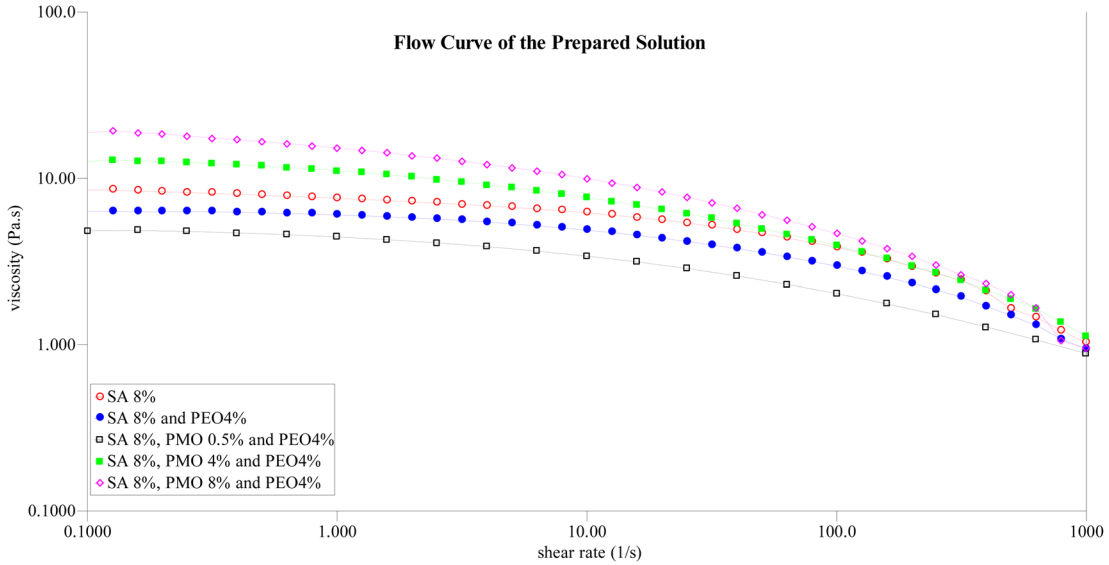

Fig. 4 Flow curve with different concentrations of pure SA, PEO, and on addition of the PMO.

evidenced by scanning electron microscopy. A deeper exploration of these rheological findings across all selected samples reveals characteristic shear-thinning or pseudoplastic behaviours with a decline in viscosity characterizes this behaviour as the shear rate Increases, indicative of an ideal polymer solution for the electrospinning process.[67] Furthermore, these solutions exhibit traits of a Newtonian plateau at minimal shear rates. This is another indication that the solution of sodium alginate contains trails of PMO for good spinnability. Higher concentrations of PMO did not lead to good homogeneous SA/PMO solutions due to the agglomeration and inherent difficulty in completing solubilizing for the electrospinning process.

4.3 Morphology of the membrane using the scanning electron microscope (SEM)

4.3.1 Effect of electric voltage on the membrane observed on (SEM). The influence of the voltage applied is one of the significant parameters as it plays an essential part in the determination of the formation of fiber morphology nature and dimensions in the electrospinning experiment.[68–70] However, it is necessary to adjust the voltage to enable a stable Taylor's cone required for the fiber formation on the surface of the collector.[71,72] In the experiments, the effect of electric voltage was observed on the addition of 0.5% PMO when the collector distance was kept constant to determine the voltage for stable Taylors' cone formation. The initial voltage was applied below 10 kV. There were no visible drops of any solution at the tip of the needle, and an increase in the voltage beyond 10 kV between 15 kV and 17 kV, caused droplets of spray beads without spun fibre on the surface of the aluminium foil collector. Further increment in voltage to 19 kV, the spinning process occurs but is not stable due to unstable and Taylor's cone cone formation at the tip of the needle. This could result in an inconsistent nanofiber formation reported by Pires *et al.*, Lin and X. Wang, also studies by Prabu and B. Dhurai.[72–74] However, our studies show that the nanofibers with varying fiber morphology were produced at a voltage between 20 kV and 24 kV to form stable Taylor's cones cone formation with more stability at between 23 kV and 24 kV with space out thinner

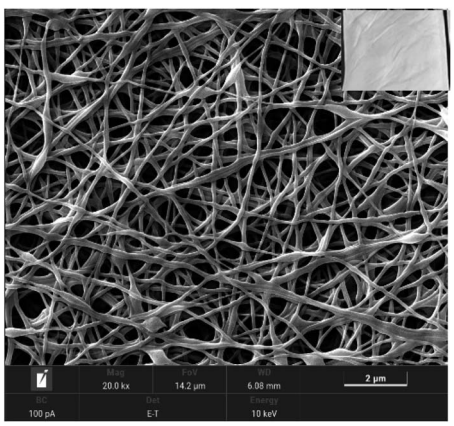

Fig. 5 SEM image of stable Taylor's cone formation of pure AMF electrospinning conditions.

Table 1 Composition of pure SA, SAF, and AMF with varying concentrations of PMO and different natures of the fiber morphology

Sample	*Moringa oleifera* (PMO) (%)	Fibre morphology	
		Beads nature	Fibre nature
A	—	No beads	Smooth
B	0.5	Spindle-like	Smooth
C	1	Spindle-like	Smooth
D	2	Spindle-like	Smooth
E	4	Spindle-like	Smooth
F	6	Spherical	Smooth
G	8	Spindle beadlike	Rough

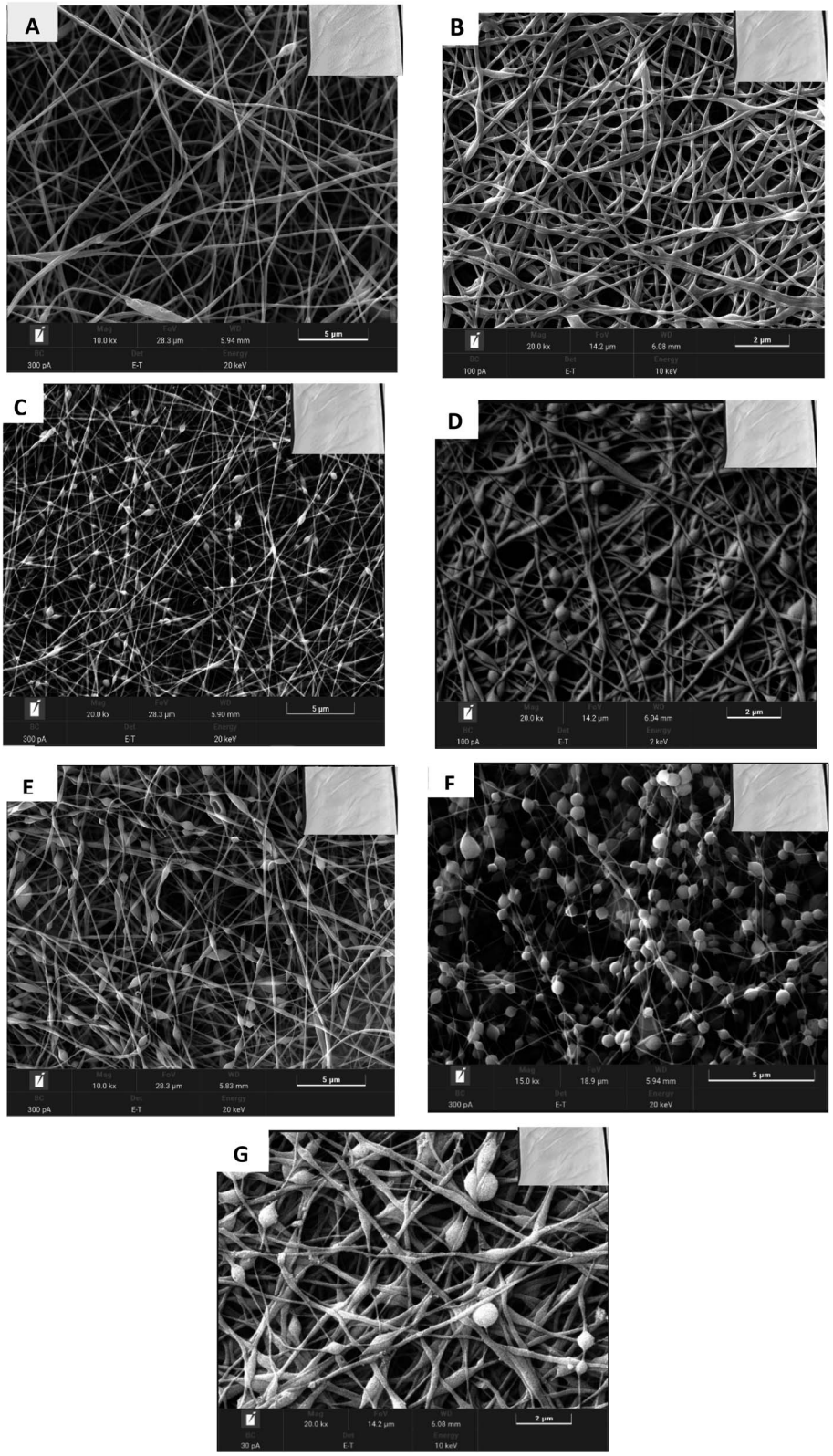

Fig. 6 SEM images of (A) pure SAF and AMF at different concentrations of (B) 0.5%, (C) 1%, (D) 2%, (E) 4%, (F) 6%, and (G) 8% of PMO.

AMF and larger encapsulated PMO described with diameter to an average of about 240 nm (±60.46) with few spindle-like pulverized *Moringa oleifera* particles bead or about 300 nm (±77.97) particle size PMO membrane as observed from the SEM presented in Fig. 5 and Table 1 respectively. However, the findings of the current study agreed with the previous studies.[37,75]

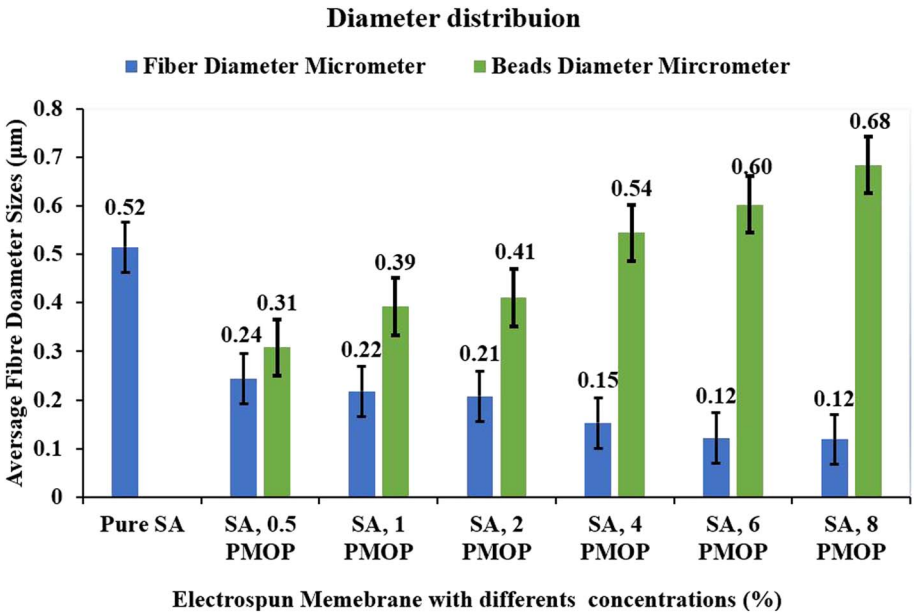

Fig. 7 Diameter distribution of AMF loaded with SA and SA loaded with PMO of different concentrations (the error bars represent the standard deviation).

4.3.2 Morphology of the pure alginate and pulverized *Moringa oleifera* on the membrane (SEM). Concentrations play a significant role in controlling fiber morphology and diameter during the electrospinning process. Different concentrations or doses of an electrospun *Moringa oleifera* were presented. The SEM morphology of the pure alginate and moringa incorporated into the alginate fiber is shown in Fig. 6A–G. The electrospun AMF was achieved with the different concentrations. Fig. 6A presents Sodium Alginate Fibre (SAF) and Fig. 6B–G are different concentrations of AMF. The result presented the addition of PMO at different concentrations resulted in considerable change in the morphology as the concentration of moringa increases beaded fibers with the presentation of spindle beadlike, spherical, smooth, or rough fiber nature as observed from the SEM image in (Table 1) as compared with pure alginate membrane (Fig. 6A) possessed a smooth fiber characteristics with an average diameter of about 515.09 nm (±114.33), the addition of different concentrations of PMO (B) 0.5%, (C) 1%, (D) 2%, (E) 4%, (F) 6%, and (G) 8% (w), presented a beaded morphology membrane with particles of *Moringa oleifera* at the addition of 0.5% PMO reduces the fiber diameter to an average of about 240 nm (±60.46) with few spindle-like pulverized *Moringa oleifera* particles bead or about 300 nm (±77.97) particle size. However, further increases or higher concentrations of the PMO reduce the fiber diameter to about 110 nm (±32.19) (8%) with the clear observation of rough spindle-like PMO particles bead of 680 nm (±131.77) particle size as shown in the histogram in Fig. 6. Similar observations occurred when Sultana and Rahman studied nanofiber composite cellulose acetate-based membrane blended with nano-zeolite.[76] Fig. 7 also shows the diameter distribution of AMF loaded with SA and SA loaded with PMO of different concentrations and the error bars represent the standard deviation indicating the increment in addition of PMO reduces the fiber diameter size. Hence, our findings on the morphology show that bead particles cannot be avoided as it is a clear indication that PMO particles have been encapsulated by SA after cross-linking. Hence the SEM morphology provides convincing evidence of PMO incorporation into the SA matrix which is in support of the FTIR results.

4.4 Thermogravimetric analysis (TGA)

The TGA analysis of SA, PMO, SAF, and AMF in the range of 25–800 °C is shown in Fig. 8. The SA powder presents a result of a different-step degradation. The first stage occurs and is observed at a temperature range between 40 and 110 °C, this

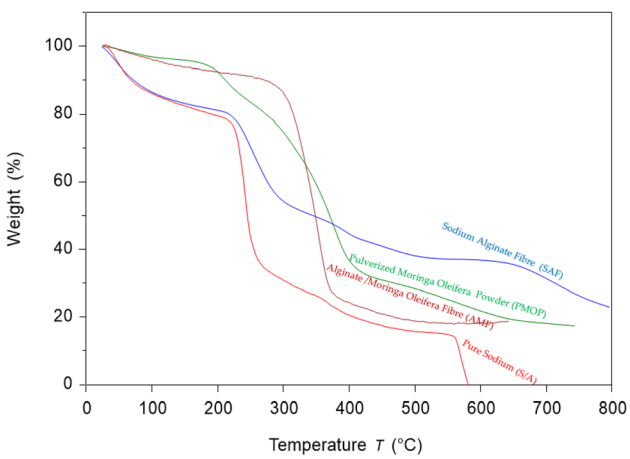

Fig. 8 TGA curves of pure SA powder, PMO, SAF, and AMF.

corresponds to the vaporization of humidity or moisture or other volatile compounds or water retention. The second step occurs between the temperature ranging from 225 to 270 °C. This is regarded as alginate degradation or decomposition of metal carbonates, which finally decomposes slowly in the third step starting beyond 570 °C. These findings agree with the previous studies by Dodero *et al.*[77] The PMO possesses three main events of weight loss the first events occur between 30 and 130 °C, this can be associated with the removal of water or water desorption, low molecular mass compounds, and volatiles compounds entrapped in the *Moringa oleifera* seeds powder. The second weight loss is allied with the removal of gases, such as CO_2 and NH_3, resulting from the presence of protein amine groups in the moringa seed powder. The third event occurs from 300 to 428 °C, which corresponds to the PMO. This study was like the previous studies by Finzi-Quintão *et al.*[78] The SAF shows some similar degradation properties, and the samples almost overlapped the profile relating to that of pure sodium alginate powders, except for the presence of an additional decomposition step, the details, show the first stage occurring at the same temperature of 40–110 °C temperature while the losses are positioned at a temperature of 330–350 °C. The degradation step can tentatively be ascribed to the crosslinking degradation property step of SA as reported by Pan *et al.*[79] which stabilizes the polymer and consequently delays its degradation. These findings are also similar as compared with studies carried out by Castellano.[80] Conclusively, the first stage of the developed AMF oleifera powder occurs at 40–130 °C which is like the first stage of the pure alginate removal of water or moisture from the membrane. While the second stage of decomposition occurs at 340–380 °C, this could be attributed to the removal of fatty acids and the presence of protein amine groups, for example, oleic acid has a boiling point of 360 °C after which it would vapor. This is like the study carried out by Bhutada *et al.*[81] on the TGA analysis of the extraction of moringa oil. This is an indication that the *Moringa oleifera* has been incorporated into the membrane as confirmed by the SEM and FTIR results discussed above.

5. Conclusion

In the current work, the electrospinning process of novel sodium alginate linked with pulverized *Moringa oleifera* seeds powder successfully produced bio-based nanofiber membranes. The result presented a notable fiber diameter reduction with the addition of various concentrations of *Moringa oleifera* concentrations between 0.5% and 8%, but concentrations exceeding 8%, altered fiber morphology during the electrospinning process. *Moringa oleifera* has been recognized for its capability of water treatment applications such as heavy metals removal and as a coagulant due to its phytochemical content. The encapsulation within sodium alginate during the electrospinning process will offer a protective solution, ensuring more stability and the prolonged release of *Moringa oleifera*'s active compounds into the water bodies as the sodium alginate biopolymer will also provide structural integrity to the developed fibers by facilitating the porosity and tunable fiber morphology. The results from The SEM morphology confirmed the successful incorporation of *Moringa oleifera* with variation in fibers and bead morphology. The FT-IR spectra confirm the presence of the amine and amide functional groups of protein content in the *Moringa oleifera* seed powder. The change in degradation properties on the addition of *Moringa oleifera* to the pure alginate is well established from the thermal study (TGA). The key findings position the nanofibers as a sustainable material for the potential application for water treatment and heavy metals adsorption.

Conflicts of interest

There is no conflict of interest in this article.

Acknowledgements

We acknowledge the Petroleum Technology Development Fund (PTDF) of the Federal Republic of Nigeria for their unwavering support in funding the Research (No. PTDF/ED/OSS/PHD/AOO/1844/2020PHD152). The financial backing has been pivotal in enabling us to conduct the essential experiments relevant to this research. The steadfast commitment to fostering human capacity and spearheading technological advancements in the Nigerian petroleum sector plays a crucial role in the success of this research. In addition, special acknowledgment is extended to Jim Hurley, senior technical officer, and all the staff of Composites and Advanced Materials Centre at Cranfield University for the invaluable technical support in ensuring the smooth progression and encouragement through significant motivation during the experimental work.

Notes and references

1 M. A. Abdulhamid and K. Muzamil, *Chemosphere*, 2023, **310**, 251–305.
2 F. Topuz, M. A. Abdulhamid, T. Holtzl and G. Szekely, *Mater. Des.*, 2021, **198**, 1–11.
3 F. Topuz, M. H. Abdellah, P. M. Budd and M. A. Abdulhamid, *Polym. Rev.*, 2024, **64**, 251–305.
4 H. M. Ibrahim and A. Klingner, *Polym. Test.*, 2020, **9**, 1–18.
5 H. Duan, H. Chen, C. Qi, F. Lv, J. Wang, Y. Liu, Z. Liu and Y. Liu, *Int. J. Pharm.*, 2024, **650**, 1–10.
6 B. Tarus, Y. Jande and K. Njau, *Water Supply*, 2024, **24**, 39–52.
7 W. S. Khan, R. Asmatulu, M. Ceylan and A. Jabbarnia, *Fibers Polym.*, 2013, **14**, 1235–1247.
8 J. Li, Q. Du, J. Wan, D.-G. Yu, F. Tan and X. Yang, *Mater. Des.*, 2024, **238**, 1–11.
9 W. S. Khan, R. Asmatulu, M. Ceylan and A. Jabbarnia, *Fibers Polym.*, 2013, **14**, 1235–1247.
10 Y. Z. Long, X. Yan, X. X. Wang, J. Zhang and M. Yu, in *Electrospinning: Nanofabrication and Applications*, ed. X. W. Bin Ding and J. Yu, William Andrew Publishing, Shanghai, 1st edn, 2019, ch. 2, vol. 1, pp. 21–52.
11 W. Wang, J. Dai, Y. Huang, X. Li, J. Yang, Y. Zheng and X. Shi, *Chem. Eng. J.*, 2023, **457**, 1–12.

12 C. Y. Su, T. Y. Liu, H. V. Wang and W. C. Yang, *Animals*, 2023, **13**, 1–13.
13 Z. Qin, T. He, C. Guo, J. Y. Kim and T. Quan, *J. Cell Commun. Signaling*, 2023, **17**, 287–296.
14 Y. Su, M. S. Toftdal, A. Le Friec, M. Dong, X. Han and M. Chen, *Small Sci.*, 2021, **1**, 1–30.
15 R. Vasita and D. S. Katti, *Int. J. Nanomed.*, 2006, **1**, 15–30.
16 F. Topuz, M. A. Abdulhamid and G. Szekely, *Chem. Eng. J.*, 2022, **449**, 137821.
17 R. Su, S. Li, W. Wu, C. Song, G. Liu and Y. Yu, *Sep. Purif. Technol.*, 2021, **256**, 117790.
18 M. R. Snowdon and R. Liang, 2018, **https://engrxiv.org/preprint/view/358**.
19 Y. Liao, C. H. Loh, M. Tian, R. Wang and A. G. Fane, *Prog. Polym. Sci.*, 2018, **77**, 69–94.
20 A. Foroozandeh, M. Shakiba, A. Zamani, A. Tajiki, M. Sheikhi, M. Pourmadadi, Z. Pahnavar, E. Rahmani, N. Aghababaei, H. S. Amoli and M. Abdouss, *J. Biomed. Mater. Res., Part B*, 2024, **112**, 1–11.
21 R. CeCe, L. Jining, M. Islam, J. G. Korvink and B. Sharma, *Adv. Eng. Mater.*, 2024, **26**, 1–18.
22 A. Dart, M. Bhave and P. Kingshott, *Macromol. Biosci.*, 2019, **19**, 1–16.
23 Z. Ren, C. Gervais and G. Singh, *RSC Adv.*, 2020, **10**, 38446–38455.
24 X. Yang, Y. Chen, C. Zhang, G. Duan and S. Jiang, *Composites, Part B*, 2023, **249**, 1–30.
25 S. Kanan, M. A. Moyet, R. B. Arthur and H. H. Patterson, *Catal. Rev.*, 2020, **62**, 1–65.
26 M. N. Chong, B. Jin, C. W. K. Chow and C. Saint, *Water Res.*, 2010, **44**, 2997–3027.
27 D. Chen, Y. Cheng, N. Zhou, P. Chen, Y. Wang, K. Li, S. Huo, P. Cheng, P. Peng, R. Zhang, L. Wang, H. Liu, Y. Liu and R. Ruan, *J. Cleaner Prod.*, 2020, **268**, 121725.
28 S. Kanan, M. A. Moyet, R. B. Arthur and H. H. Patterson, *Catal. Rev.: Sci. Eng.*, 2020, **62**, 1–65.
29 S. Thakur, J. Chaudhary, P. Singh, W. F. Alsanie, S. A. Grammatikos and V. K. Thakur, *Bioresour. Technol.*, 2022, **344**, 1–10.
30 J. Gutierrez-Gonzalez, E. Garcia-Cela, N. Magan and S. S. Rahatekar, *Mater. Lett.*, 2020, **270**, 1–4.
31 T. A. Saleh, M. Mustaqeem and M. Khaled, *Environ. Nanotechnol., Monit. Manage.*, 2022, **17**, 1–14.
32 T. T. Li, Y. Zhong, M. Yan, W. Zhou, W. Xu, S. Y. Huang, F. Sun, C. W. Lou and J. H. Lin, *Nanomaterials*, 2019, **9**, 714.
33 T. C. Mokhena, M. J. Mochane, A. Mtibe, M. J. John, E. R. Sadiku and J. S. Sefadi, *Materials*, 2020, **13**, 1–24.
34 H. M. El-Husseiny, E. A. Mady, A. S. Doghish, M. B. Zewail, A. M. Abdelfatah, M. Noshy, O. A. Mohammed and W. A. El-Dakroury, *Int. J. Biol. Macromol.*, 2024, **260**, 1–30.
35 S. Safi, M. Morshed, S. A. Hosseini Ravandi and M. Ghiaci, *J. Appl. Polym. Sci.*, 2007, **104**, 3245–3255.
36 J. W. Lu, Y. L. Zhu, Z. X. Guo, P. Hu and J. Yu, *Polymers*, 2006, **47**, 8026–8031.
37 H. Lu, J. A. Butler, N. S. Britten, P. D. Venkatraman and S. S. Rahatekar, *Nanomaterials*, 2021, **11**, 1–16.
38 A. D. Juncos Bombin, N. J. Dunne and H. O. McCarthy, *Mater. Sci. Eng., C*, 2020, **114**, 1–16.
39 R. Wongkanya, P. Chuysinuan, C. Pengsuk, S. Techasakul, K. Lirdprapamongkol, J. Svasti and P. Nooeaid, *J. Sci.: Adv. Mater. Devices*, 2017, **2**, 309–316.
40 A. Pareek, M. Pant, M. M. Gupta, P. Kashania, Y. Ratan, V. Jain, A. Pareek and A. A. Chuturgoon, *Int. J. Mol. Sci.*, 2023, **24**, 1–36.
41 P. Garg, S. Pundir, A. Ali, S. Panja, D. K. Chellappan, K. Dua, S. Kulshrestha and P. Negi, *Naunyn-Schmiedeberg's Arch. Pharmacol.*, 2023, **1**, 1–28.
42 K. Gharsallah, L. Rezig, M. S. R. Rajoka, H. M. Mehwish, M. A. Ali and S. C. Chew, *S. Afr. J. Bot.*, 2023, **160**, 180–193.
43 A. N. Jikah and G. I. Edo, *J. Sci. Food Agric.*, 2023, **103**, 7343–7361.
44 N. Ueda Yamaguchi, F. Cusioli, H. B. Quesada, M. Eliana, C. Ferreira, R. Fagundes-Klen, A. Marquetotti, S. Vieira, R. G. Gomes, M. Fernandes Vieira and R. Bergamasco, *Process Saf. Environ. Prot.*, 2021, **147**, 405–420.
45 N. Al-Jadabi, M. Laaouan, S. El Hajjaji, J. Mabrouki, M. Benbouzid and D. Dhiba, *Sustainability*, 2023, **15**, 1–37.
46 R. S. Gambhir, V. Kapoor, A. Nirola, R. Sohi and V. Bansal, *Hum. Ecol.*, 2012, **37**, 103–109.
47 A. Abiyu, D. Yan, A. Girma, X. Song and H. Wang, *Cogent Environ. Sci.*, 2018, **4**, 1–13.
48 C. S. T. Araújo, E. I. Melo, V. N. Alves and N. M. M. Coelho, *J. Braz. Chem. Soc.*, 2010, **21**, 1727–1732.
49 R. Bouchareb, K. Derbal and A. Benalia, *Water Sci. Technol.*, 2021, **84**, 393–403.
50 R. Silva, B. Bulut, J. A. Roether, J. Kaschta, D. W. Schubert and A. R. Boccaccini, *J. Mol. Struct.*, 2014, **1073**, 87–96.
51 T. Elo, V. S. Parihar, A. Bera, F. Javanshour, M. Kellomäki and R. Layek, *Colloids Surf., B*, 2024, **233**, 1–9.
52 S. A. Sideek, H. B. El-Nassan, A. R. Fares, N. A. Elkasabgy and A. N. ElMeshad, *Pharmaceutics*, 2024, **16**, 1–30.
53 D. Dehnad, B. Ghorani, B. Emadzadeh, F. Zhang, N. Yang and S. M. Jafari, *Food Hydrocolloids*, 2024, **151**, 1–16.
54 G. A. Bhat, P. Vishnoi, S. K. Gupta and R. Murugavel, *Inorg. Chem. Commun.*, 2015, **59**, 84–87.
55 P. Devgupta, P. K. Pramanik, D. Roy Chowdhury, P. Ghosh and T. Chakraborti, *J. Herb. Med.*, 2024, **43**, 1–10.
56 M. Banerjee and V. D. Rajeswari, *Biocatal. Agric. Biotechnol.*, 2024, **55**, 1–21.
57 I. M. Militao, F. Roddick, R. Bergamasco and L. Fan, *Environ. Technol. Innovation*, 2022, **28**, 1–13.
58 A. A. H. Abdellatif, M. A. Ibrahim, M. A. Amin, H. Maswadeh, M. N. Alwehaibi, S. N. Al-Harbi, Z. A. Alharbi, H. A. Mohammed, A. B. M. Mehany and I. Saleem, *Sci. Rep.*, 2020, **10**, 1–14.
59 C. Niemi, J. Takahashi, A. Gorzsás and F. G. Gentili, *Int. J. Biol. Macromol.*, 2024, **254**, 1–8.
60 P. Tordi, R. Gelli, F. Ridi and M. Bonini, *Carbohydr. Polym.*, 2024, **326**, 1–11.
61 A. L. Mutch, V. Ferro, A. Anitha and L. Grøndahl, *Carbohydr. Polym.*, 2024, **324**, 1–19.

62 H. M. A. Haseef, S. Dinesh, J. Prakash, M. S. Marvaan, S. Madasamy, B. Pannerselvam and G. D. Venkatasubbu, *Int. J. Biol. Macromol.*, 2024, **254**, 1–14.
63 R. Kannan, S. Lakshmi, N. Aparna, S. Prabhakar and W. R. Thilagaraj, *Int. J. Ind. Chem.*, 2016, **7**, 265–275.
64 Q. Zhang, J. Lin, Y. Dong and F. Sun, *Colloids Surf., A*, 2023, **661**, 1–13.
65 G. Akhouy, K. Aziz, L. Gebrati, M. El Achaby, Y. Akgul, P.-S. Yap, T. Agustiono Kurniawan and F. Aziz, *Polym.-Plast. Technol. Mater.*, 2023, **62**, 1754–1775.
66 S. Sattariazar, S. Nejad Ebrahimi and N. Arsalani, *Int. J. Pharm.*, 2023, **644**, 1–9.
67 J. Mirtič, H. Balažic, Š. Zupančič and J. Kristl, *Polymers*, 2019, **11**, 2–20.
68 R. V. N. Krishnappa, *J. Mater. Sci.*, 2003, **38**, 2357–2365.
69 Y. Liu, J. Chen, V. Misoska and G. G. Wallace, *React. Funct. Polym.*, 2007, **67**, 461–467.
70 C. Du, Z. Wang, G. Liu, W. Wang and D. Yu, *Colloids Surf., A*, 2021, **624**, 1–10.
71 N. Shirai, R. Sekine, S. Uchida and F. Tochikubo, *Jpn. J. Appl. Phys.*, 2014, **53**, 026001.
72 J. B. Pires, F. N. dos Santos, I. H. d. L. Costa, D. H. Kringel, E. d. R. Zavareze and A. R. G. Dias, *Food Res. Int.*, 2023, **170**, 112970.
73 H. Niu, T. Lin and X. Wang, *J. Appl. Polym. Sci.*, 2009, **114**, 3524–3530.
74 G. T. V. Prabu and B. Dhurai, *Sci. Rep.*, 2020, **10**, 1–11.
75 H. Fong, I. Chun and D. H. Reneker, *Polymers*, 1999, **40**, 4585–4592.
76 N. Sultana and R. Rahman, *Emergent Mater.*, 2022, **5**, 145–153.
77 A. Dodero, M. Alloisio, S. Vicini and M. Castellano, *Carbohydr. Polym.*, 2020, **227**, 1–8.
78 C. M. Finzi-Quintão, K. M. Novack, A. C. Bernardes-Silva, T. D. Silva, L. E. S. Moreira and L. E. M. Braga, *Environ. Technol.*, 2019, **40**, 508–517.
79 Y. Pan, W. Wang, L. Liu, H. Ge, L. Song and Y. Hu, *Carbohydr. Polym.*, 2017, **170**, 133–139.
80 M. Castellano, M. Alloisio, R. Darawish, A. Dodero and S. Vicini, *J. Therm. Anal. Calorim.*, 2019, **137**, 767–778.
81 P. R. Bhutada, A. J. Jadhav, D. V. Pinjari, P. R. Nemade and R. D. Jain, *Ind. Crops Prod.*, 2016, **82**, 74–80.